Robustness of laser phase fronts in backward Raman amplifiers

G. M. Fraiman,[a] N. A. Yampolsky, V. M. Malkin, and N. J. Fisch
Department of Astrophysical Sciences, Princeton University, Princeton, New Jersey 08544

(Received 14 February 2002; accepted 7 May 2002)

The backward Raman amplification (BRA) of short laser pulses in plasma is studied numerically in two space dimensions. A high quality prefocused seed pulse is shown to remain well-focused through the entire process of the seed amplification by a high quality pump. In addition, it is shown that the BRA is not sensitive to a broad class of pump and seed fluctuations. The BRA length at which self-focusing and self-phase-modulation effects appear is determined numerically. © *2002 American Institute of Physics.* [DOI: 10.1063/1.1491959]

I. INTRODUCTION

The fast compression (FC) of laser pulses by means of stimulated backward Raman scattering (SBRS) in plasma has been proposed in Ref. 1 as a means to reach ultrahigh laser powers. In the FC scheme, a short seed pulse consumes essentially all of a long incident pump power and contracts as its amplitude grows. The amplification/compression is fast enough to reach nearly relativistic pumped pulse intensities, like $10^{17}\,\mathrm{W/cm^2}$ for $\lambda=1\ \mu$m-wavelength radiation, within times shorter than it takes for filamentation instabilities to develop. Such a nonfocused intensity would be 10^5 times higher than currently available through the chirp pulse amplification (CPA) technique (see, for instance, Ref. 2). For shorter wavelength lasers, this factor would be even higher (see Refs. 1 and 3).

Our major goal in the current work is to examine the output pulse transverse quality, which is important for the focusability of the output pulse. Even if the full amplification within the plasma is obtained, the pulse must emerge from the plasma with a high quality front in order for the full vacuum focusing to be achieved as well.

The paper is organized as follows: First, we show that a convergent phase front of the seed pulse can maintain its shape during the amplification. Then, we show that amplitude modulations of seed pulse in the transverse direction are smoothed during the nonlinear stage of BRA. We show next that the pump phase fluctuations do not affect the pulse amplification and phase fronts over a broad range of parameters, but rather are mirrored by the phase of Langmuir wave that mediates the energy transfer from pump to pulse. Similarly, in a broad parameter range, the pump intensity fluctuations are averaged over by the seed pulse, with no significant change in the pulse amplification and phase fronts. Finally, we determine numerically the largest amplification length and pumped pulse intensity for which self-focusing and self-phase-modulation effects are not yet significant.

II. BASIC EQUATIONS

The equations for the precisely resonant backward Raman amplification (BRA), taking into account the transverse dispersion and self-focusing nonlinearity of the pumped pulse, can be put in the form (see, for instance, Refs. 4 and 5)

$$a_t + c a_z = -Vfb, \quad V=\sqrt{\omega\omega_p/2}, \tag{1}$$

$$b_t - c b_z = Vaf^* - i\frac{c^2}{2\omega}\Delta_\perp b - i\frac{\omega_p^2}{4\omega}|b|^2 b, \tag{2}$$

$$f_t = Vab^*. \tag{3}$$

Here ω_p is the electron plasma frequency, $\omega \gg \omega_p$ is the laser frequency, a and b are the dimensionless space–time envelopes of, respectively, the pump and the seed electron quiver velocities, normalized so that the pump power density is $I_a = \pi c(m_e c^2/e)^2|a|^2/\lambda^2 = 2.736\times 10^{18}|a|^2/\lambda^2(\mu\mathrm{m})\ \ \mathrm{W/cm^2}$, with a similar normalization for the seed b, while f is the appropriately normalized Langmuir wave envelope; λ is the laser wavelength, t is the time, z is the distance in the direction of the pump propagation, subscripts denote the respective derivatives, and c is the vacuum speed of light.

These equations assume, in particular, that the characteristic spatial scales of the wave envelopes are much larger than the laser wavelength, and the characteristic times of the wave envelopes are much larger than the inverse plasma frequency. The transverse dispersion term (containing the transverse Laplacian $\Delta_\perp$) is taken into account only for the seed pulse, because the pump passes through or is consumed by the seed too fast to manifest the diffraction effects within the seed location, and it is only the seed development that interests us here. The relativistic electron nonlinearity is also taken into account only for the seed pulse, because the seed is ultimately amplified to intensities much higher than that of the pump.

In rescaled dimensionless variables,

$$\tau = Vt, \quad \zeta = V(t+z/c), \quad \vec{\rho} = \sqrt{2\omega V}\vec{r}_\perp/c, \tag{4}$$

the basic equations take the form

$$2a_\zeta + a_\tau = -bf, \tag{5}$$

$$b_\tau = af^* - i\Delta_\rho b - i\delta|b|^2 b, \quad \delta = (\omega_p/2\omega)^{3/2}, \tag{6}$$

$$f_\zeta + f_\tau = ab^*, \tag{7}$$

where Δ_ρ is the transverse Laplacian in variable $\vec{\rho}$. In Secs. III–VI, we neglect the relativistic electron nonlinear-

[a]Permanent address: Institute of Applied Physics, Russian Academy of Sciences, Nizhnii Novgorod, 603950, Russia.

ity and solve the basic equations with $\delta=0$. In Sec. VII, evaluating self-focusing and self-phase-modulation effects, we solve the basic equations with finite δ.

For $\delta=0$, the basic equations are invariant to the transformation $a\to Ca$, $b\to Cb$, $f\to Cf$, $\tau\to\tau/C$, $\zeta\to\zeta/C$, $\vec{\rho}\to\vec{\rho}/\sqrt{C}$ with an arbitrary constant $C>0$. Therefore, the specific value of the pump amplitude a_0 selected below is not in fact important in the sense that the field dynamics for different a_0 can be obtained by a simple rescaling. Note, however, that this is so just in the framework of such a simple mathematical model, not taking into account effects of self-focusing, Langmuir wave breaking, etc. At the thresholds for the appearance of these other effects the numerical solution of the simplest model should be a crude enough approximation to real dynamics (see, for instance, a comparison of hydrodynamic and kinetic calculations near threshold of the Langmuir wave breaking regime in Ref. 1). Yet, for wave amplitudes well under the thresholds, the simplest model is sufficiently accurate. Then, the BRA dynamics is independent of the pump amplitude up to the above rescaling. Note that this rescaling affects, in particular, the pumped pulse energy. To get the same pumped pulse energy for C^2 times more intense pump, the C^2 shorter distance is needed, since the pump is completely consumed.

III. NUMERICAL SETUP

The above equations were solved numerically in a two-dimensional model containing just one transverse coordinate, $\vec{r}_\perp=\vec{e}_y y$. The numerical scheme employed the operator exponent method with fast Fourier transform in the transverse direction for solving the parabolic equation, the method of characteristics for solving hyperbolic equations, and an implicit scheme for accounting for nonlinear interactions within each time step.

The numerical calculations were performed in a z-window moving together with the seed pulse. The calculations started at the instant $t=0$ when the pump has already entered the window, but has not yet collided with the seed. The initial z-dependence of the seed was typically taken Gaussian,

$$b(t=0,z,y)=\exp\left[-\left(\frac{z-z_0}{\Delta z}\right)^2\right]\frac{c\varepsilon(y)}{V\sqrt{\pi}\Delta z}. \tag{8}$$

The pump front was initially (i.e., at $t=0$) located at $z=0$ and well-separated from the seed, for $z_0\gg\Delta z$. The left boundary of the computational z-window was initially located at $z=0$, and then moved with speed $-c$, so that it was located at $z=-ct$ and remained well-separated from the amplified seed. The pump, entering the computational z-window at $z=-ct$, was considered as a given external function,

$$a(t,z=-ct,y)=a_0A(t,y)\Theta(t),$$
$$(\Theta(t)=1,\ t>0,\ \Theta(t)=0,\ t<0,\ A\sim 1). \tag{9}$$

In the runs presented below, we typically used

$$a_0=0.0085,\ \omega/\omega_p=12,\ z_0=60\lambda,\ \Delta z=6\lambda. \tag{10}$$

As was already noted, the value of a_0 can be removed from the simplest model by a rescaling. We fix a_0 here primarily to fix the amplification distance in the numerical examples with $\delta=0$ that follow. All these examples present the universal (a_0-independent) dynamics within the simplest model, even though the selected a_0 belongs, in fact, to the wave-breaking region that, strictly speaking, requires a kinetic description.

The initial seed amplitude, integrated over z,

$$\int b(t=0,\ z=\zeta c/V,\ y)d\zeta=\varepsilon(y), \tag{11}$$

was taken moderately small, $\varepsilon\sim 0.1$. Note that the integrated initial seed amplitude thus defined, ε, differs by the factor $\sqrt{2}$ from the integrated initial seed amplitude $\epsilon_{\rm old}$ used in Ref. 1,

$$\epsilon_{\rm old}=\sqrt{2}\,\varepsilon. \tag{12}$$

In some of the plots presented below, we show for comparison the one-dimensional (1D) π-pulse amplification regime, where the transverse dispersion and focusing cubic nonlinearity are neglected.[1] For the pulse duration much smaller than the pulse amplification time (which is so for an advance nonlinear amplification stage), the terms f_τ and a_τ also can be neglected. Then, for a real constant pump, $A=1$, there is a solution of the form

$$a=a_0\cos(u/2),\ \ f=\sqrt{2}a_0\sin(u/2),\ \ b=u_\zeta/\sqrt{2}, \tag{13}$$

where u satisfies the sine-Gordon equation,

$$u_{\tau\zeta}=a_0^2\sin u. \tag{14}$$

It has a family of self-similar solutions $u(\tau,\zeta)=U(\eta=a_0^2\tau\zeta)$, where U solves the ordinary differential equation solution,

$$\eta U_{\eta\eta}+U_\eta=\sin U, \tag{15}$$

and depends on a single parameter $U(+0)=\epsilon_{\rm old}$.

The length of the initial seed pulse Δz is chosen small enough to avoid an early decrease in effective ε, which occurs when the leading amplified spike of π-pulse (moving with a super-luminous velocity) overtakes the maximum of the original seed (that moves with the speed of light). A short initial seed is also favorable for suppression of the deleterious superluminous precursors as described in Ref. 6. On the other hand, the length of the initial seed pulse Δz is chosen large enough to allow the use of the wave envelope equations. The most restrictive condition on these equations occurs for the time envelope of the resonant Langmuir wave, because the Langmuir wave frequency is much smaller than the laser frequencies. In particular, this condition implies that the initial seed duration exceeds ω_p^{-1}.

We neglect the dispersion of the longitudinal group velocity. This dispersion is small, and does not cause a significant stretching of the original seed up to the propagation distance,

$$L_{\rm str}\sim\lambda(\omega\Delta z/\omega_p\lambda)^2, \tag{16}$$

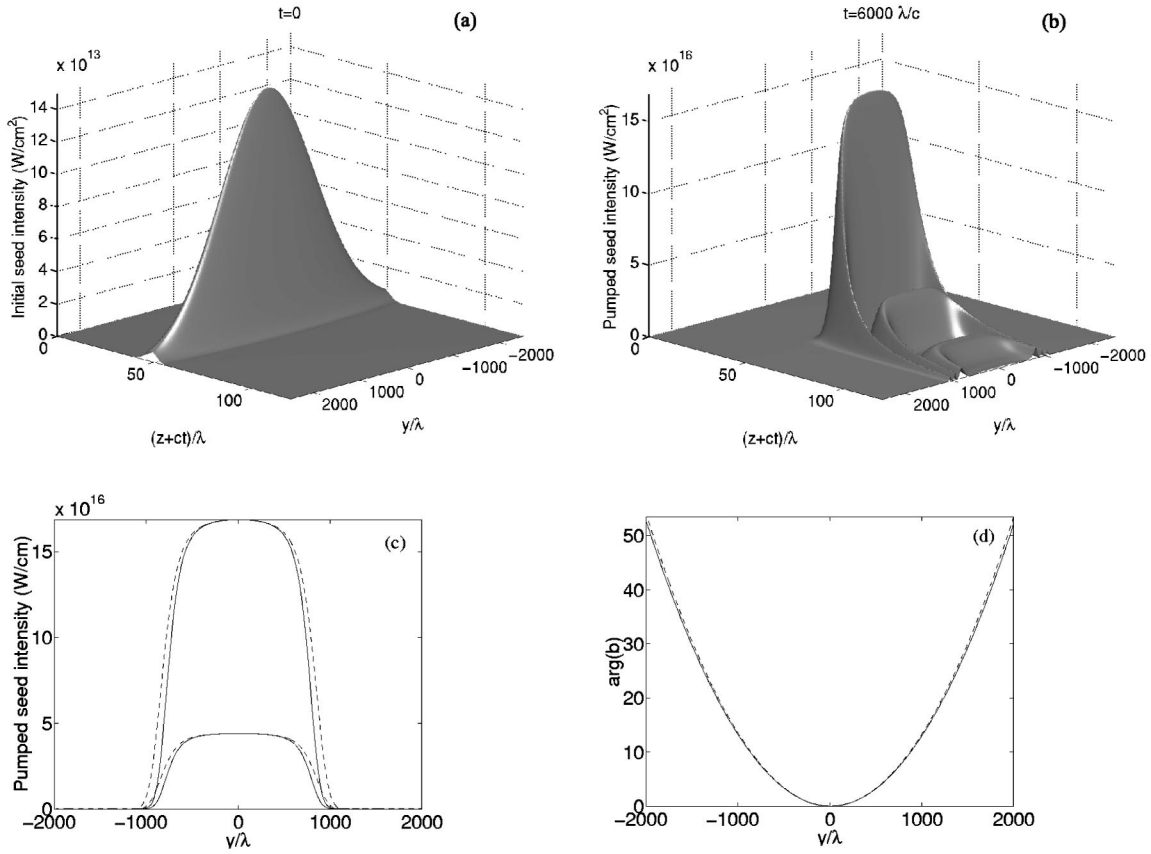

FIG. 1. Backward Raman amplification of the prefocused seed. (a) The distribution of the initial seed intensity; (b) the distribution of the pumped (about 1000 times) seed intensity at $t=6000\lambda/c$; (c) the transverse dependence of the pumped pulse intensity at the z-location of the absolute maximum of the pulse intensity at times $t=3000\lambda/c$ and $t=6000\lambda/c$ (solid lines). The respective dashed lines show the transverse dependence of pulse intensity maximum over z, found separately for each y, at the same times; (d) the transverse dependence of the pumped pulse phase fronts for z corresponding to the absolute maximum of the pulse intensity at the times $t=0$ (solid line) and $t=6000\lambda/c$ (dashed line).

which gives for the above numbers $L_{\mathrm{str}}\sim 5000\lambda$. The diffraction effects are relatively small up to the propagation distance,

$$L_{\mathrm{diffr}}\sim \pi(\Delta y)^2/\lambda, \tag{17}$$

where Δy is a spatial scale in the transverse direction of the pumped pulse.

IV. PREFOCUSED SEED AMPLIFICATION

One may expect that a high quality prefocused seed pulse maintains the convergent shape of its phase fronts when amplified by a high quality pump. The reason for this is as follows: The leading part of seed pulse has a small intensity and propagates nearly in the linear regime, provided that the seed front encounters quiet fresh plasma, where Langmuir waves, that might couple the seed to the pump, are not yet excited. Then, the convergent (say parabolic) shape of phase fronts is conserved for this low intensity leading part of seed. The resonant Langmuir wave excitation and pump backscattering initiated by this leading part of seed amplify succeeding layers of the pumped pulse. Thus, the most intense part of the pumped pulse likely propagates along the rays basically determined by the phase front shape of the low intensity original seed, which is always ahead of the major pumped layers of the pulse. (Note, that differently shaped phase fronts are also likely maintain their shapes when diffraction effects are small, but we are interested here specifically in convergent fronts.)

To verify this numerically, we calculated BRA for the above setup with

$$\varepsilon(y)=0.1\exp\left(-\frac{y^2}{(\Delta y)^2}+i\frac{\pi y^2}{2\lambda F}\right),$$

$$F=120000\,\lambda, \quad \Delta y=2000\,\lambda, \tag{18}$$

$$A(t,y)=[\tanh((y/\lambda+1000)/100) - \tanh((y/\lambda-1000)/100)]/2. \tag{19}$$

In this numerical calculation, the seed has parabolic phase fronts. The focusing length F is much larger than the length of amplification. The results shown in Fig. 1 confirm that the parabolic phase front maintains its shape during the amplification, behaving like during the vacuum propagation. The diffraction effects are small, and for each optical ray the 1-D self-similar solution sets up. The pump is completely consumed, as long as the initial seed is broader than the pump in the transverse direction. The peak pulse intensity then becomes more flat in the transverse direction. This is because

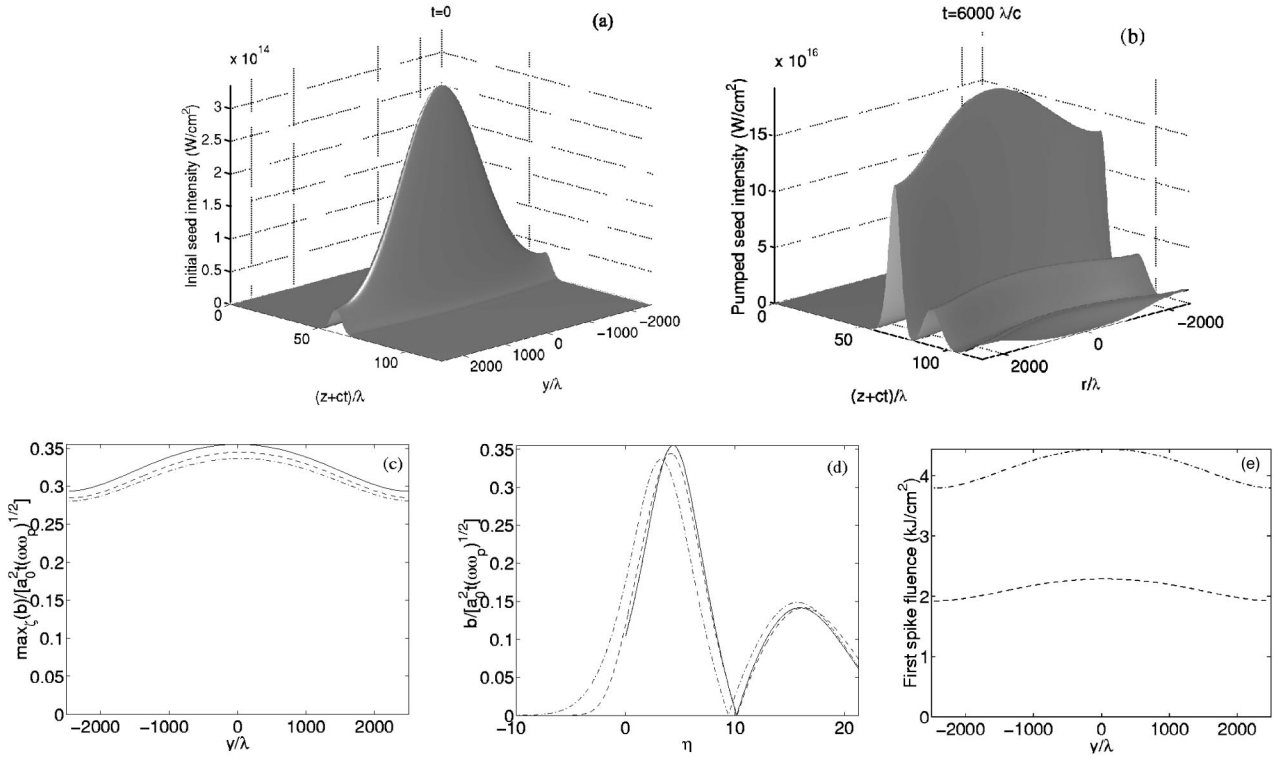

FIG. 2. Backward Raman amplification of the quasi-plain seed with transverse-modulated amplitude. (a) The distribution of the initial seed intensity; (b) the distribution of the pumped seed intensity at $t=6000\lambda/c$; (c) transverse dependence of the appropriately rescaled leading spike maximum at times $t=3000\lambda/c$ (dashed line) and $t=6000\lambda/c$ (dash–dotted line) in comparison with the self-similar π-pulse solution (solid line); (d) longitudinal dependence of the pumped pulse rescaled amplitude at $y=0$ at times $t=3000\lambda/c$ (dashed line) and $t=6000\lambda/c$ (dash–dotted line) in comparison with the self-similar solution π-pulse solution (solid line); (e) transverse dependence of the leading spike fluence at times $t=3000\lambda/c$ (dashed line) and $t=6000\lambda/c$ (dash–dotted line).

the consumed pump intensity has a flat transverse dependence. The remaining transverse dependence of the peak pulse intensity is associated with a weak (logarithm) dependence of the 1-D self-similar solution on the initial integrated amplitude ε. At the transverse edges, the pumped pulse intensity drops even more sharply than that of the pump. The steep drop is caused by the quadratic dependence of pumped pulse intensity on pump intensity in the π-pulse self-similar amplification/compression regime where $b\propto a_0^2 t$. That is why pulse width at half the maximum intensity is approximately the same as the pump width at 3/4 of the maximum intensity.

Figure 1(c) shows the transverse dependence of the pumped pulse intensity for the z-location of the absolute maximum of the pulse intensity at times $t=3000\lambda/c$ and $t=6000\lambda/c$ (solid lines). The respective dashed lines show the transverse dependence of the pulse intensity maximum over z, found separately for each y, at the same times. The solid and dashed lines are close to each other inside the energy-containing area. It means that the intensity front is nearly plane.

Figure 1(d) shows the transverse dependence of the pumped pulse phase fronts of the pulse in the transverse direction for z corresponding to the absolute maximum of the pulse intensity at the times $t=0$ (solid line) and $t=6000\lambda/c$ (dashed line). The small change of the phase front is caused by a small front advance towards the focal point; this change is the same as in vacuum.

Based on these results we consider further, for simplicity, just quasi-plane fragments of seed pulse fronts. Within such a fragment, the seed phase is nearly constant and can be made zero by a simple change of notations. Consider therefore possible amplitude modulation of the seed within a quasi-plane fragment of the front.

V. AMPLITUDE MODULATION OF SEED

One might expect that transverse amplitude modulations of a short quasi-plane seed are smoothed during the nonlinear stage of BRA. This is because the 1-D π-pulse attractor solution depends on just a single parameter ε, and this dependence is logarithmic, which is a smooth function for small ε. Note, that, since the pump is completely depleted, the same amount of pump energy is deposited in rays that might have much different ε. Depending on ε, this energy is, however, somewhat differently distributed between the leading and the succeeding spikes of the pumped π-pulse wavetrain. The results of numerical calculations with initial data,

$$\varepsilon(y)=0.1\left(1+0.5\cos\left(2\pi\frac{y}{\Delta y}\right)\right),\quad \Delta y=5000\lambda,\quad A(t,y)=1, \tag{20}$$

are shown in Figs. 2. The transverse scale of this modulation

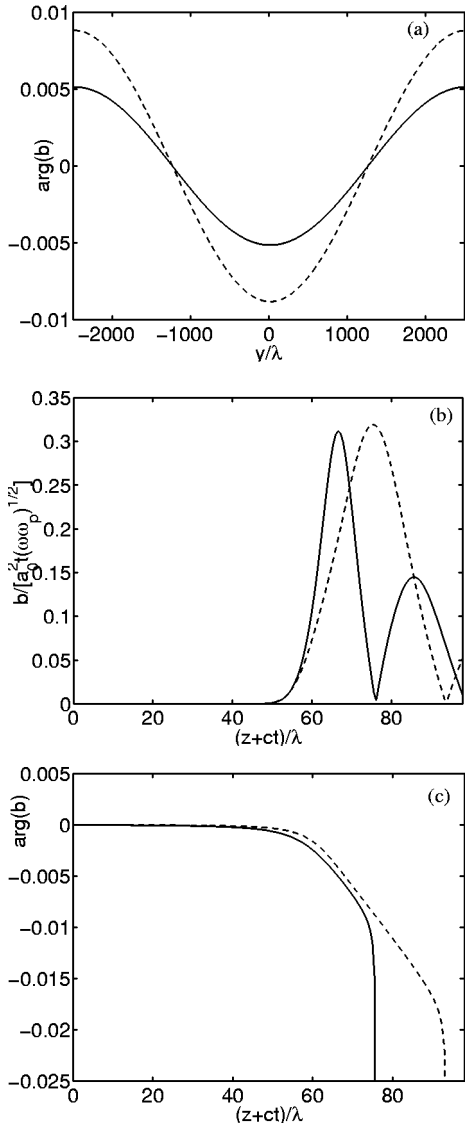

FIG. 3. (a) The transverse phase dependence of the pumped pulse for the z-location of the absolute maximum of the pulse intensity at times $t=3000\lambda/c$ (dashed line) and $t=6000\lambda/c$ (solid line). This phase modulation is smaller than 0.01 and it becomes smaller yet during the amplification process. (b) The longitudinal dependence of the rescaled amplitude of the pumped pulse for $y=0$ at the same times. (c) The longitudinal phase dependence of the pumped pulse for $y=0$ at the same times. The phase perturbation tends to increase sharply in the vicinity of the points of small pulse amplitude $b\approx 0$, but there just a negligible energy is located. The energy containing domain is very little affected: as seen, the pulse acquires there a very small frequency shift.

is large enough for diffraction effects to be negligible. The output pulse indeed has substantially smaller amplitude modulation at the time $t=6000\lambda/c$ when the duration of the linear BRA stage is already relatively small compared to the duration of the nonlinear BRA stage.

Figure 2(c) shows the transverse dependence of the appropriately rescaled leading spike maximum at times $t=3000\lambda/c$ (dashed line) and $t=6000\lambda/c$ (dash–dotted line) in comparison with the self-similar π-pulse solution (solid line). The small difference is due to a small decrease of effective integrated seed amplitude $\varepsilon_{\mathrm{eff}}$ caused by the pumped spike entering into the trailing domain of the initial seed. As seen, the leading spike amplitude varies in the transverse direction just by 15%, while initially (at $t=0$) this variation was by 3 times. For a smaller ε, the smoothening effect would be even stronger.

Figure 2(d) shows the longitudinal dependence of the pumped pulse rescaled amplitude at $y=0$ at times $t=3000\lambda/c$ (dashed line) and $t=6000\lambda/c$ (dash–dotted line) in comparison with the self-similar solution π-pulse solution (solid line), $\eta=a_0^2\tau\zeta$. The small difference is due to a small decrease of $\varepsilon_{\mathrm{eff}}$.

Figure 2(e) shows the transverse dependence of the leading spike fluence at times $t=3000\lambda/c$ (dashed line) and $t=6000\lambda/c$ (dash–dotted line). The pump that meets the seed before the time $t=6000\lambda/c$ carries fluence $W=8$ kJ/cm^2. As seen, about half of this fluence goes to the leading spike.

VI. PUMP FLUCTUATIONS

Consider, first, phase fluctuations of the pump. An absolute value of the pump phase affects just the phase of Langmuir wave resonantly excited by the pump and seed. It does not affect the phase of the amplified seed and, therefore, is not important here. The pump phase gradients, however, imply a detuning of the 3-wave resonance, which can affect BRA. The effect of a regular resonance detuning on BRA was analyzed and usefully employed in Ref. 7. Here, we are concerned primarily in random phase fluctuations and gradients. One can assume that, as long as the detuning is small, these random effects are basically averaged and thus are not important over a broad parameter range.

To verify this, we solved numerically our basic equations with the initial and boundary conditions,

$$\varepsilon(y)=0.1,$$

$$A(t,y)=\exp\left(i\pi\cos\left(2\pi\frac{y}{\Delta y}\right)\cos\left(\frac{\omega t}{N}\right)\right),$$

$$\Delta y=5000\lambda, \quad N=1200. \tag{21}$$

This example considers both the longitudinal and the transverse fluctuations of the pump phase. The results, shown in Fig. 3, indicate that the BRA is indeed very little affected by even large phase fluctuations of the pump that do not cause too much detuning. The transverse profile of the pumped pulse maximum intensity is not shown, because it remains essentially uniform. There is a small transverse modulation of the pumped pulse phase. The resulting field can be viewed as a nearly linear superposition of a large transverse-uniform field and a small transverse-modulated field. The latter should not cause, however, significant energy loss, as long as the regular amplified field can be effectively focused to a small spot in the vacuum focusing following the BRA.

Consider now intensity fluctuations of the pump, assuming that accompanying phase fluctuations are not important and hence can be ignored.

One may expect that the pump intensity fluctuations are averaged during the amplification process, as it occurs in traditional BRA (see Ref. 8). This is because the amplified pulse consumes the pump (moving towards it with the speed

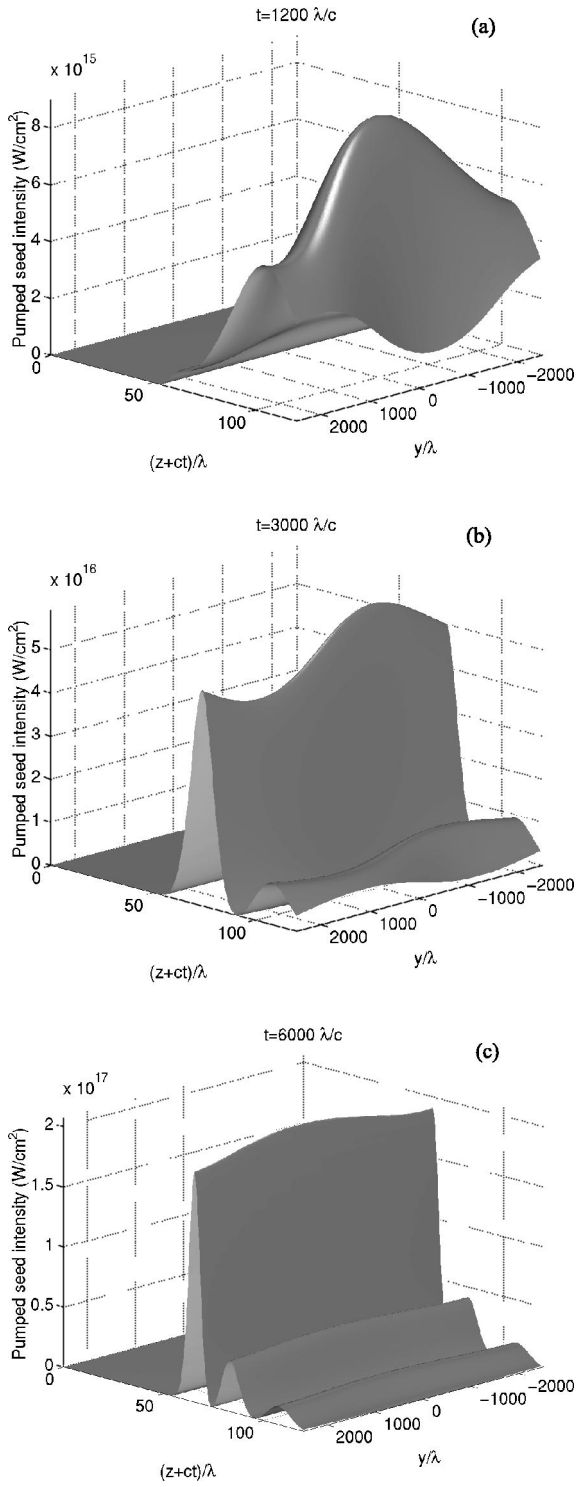

FIG. 4. The pumped seed pulse evolution during the backward Raman amplification by the pump of a fluctuating intensity. Even under unfavorable conditions when the duration of fluctuations exceeds the linear amplification time, the fluctuations are ultimately averaged.

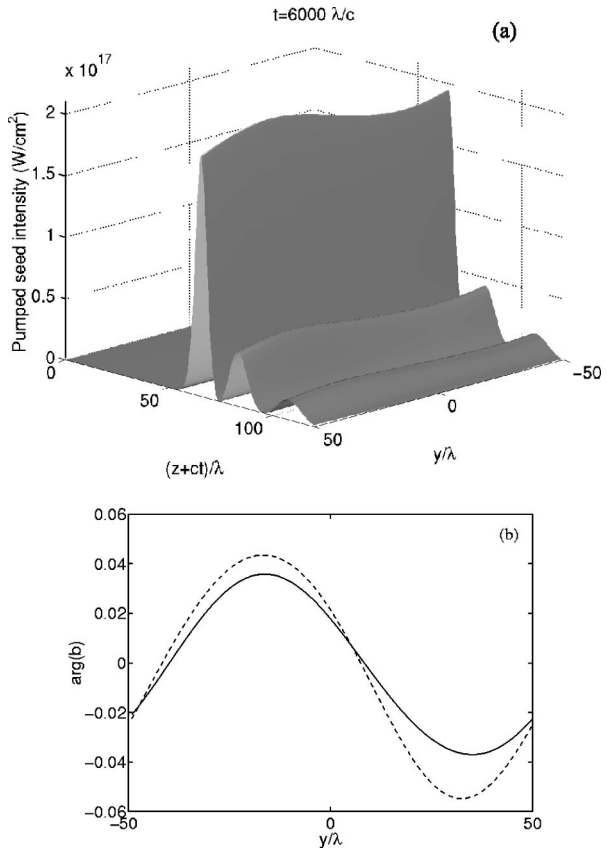

FIG. 5. The pumped seed pulse evolution as in Fig. 4, except that the transverse scale of the pump fluctuations $\Delta y = 100\lambda$ is 50 times smaller. Note that diffraction produces some phase modulations of the pumped pulse from its pump-induced amplitude modulations. (b) The transverse dependence of the phase modulations for the z-location of the maximum pulse intensity at times $t = 6000\lambda/c$ (solid line) and $t = 3000\lambda/c$ (dashed line). Note that these modulations do not decrease in time.

$2c$), so that the fluence of the pump meeting the pulse is important rather than the pump intensity at each time instant.

For effective averaging, the typical duration of the pump fluctuations should be much smaller than the typical amplification time. This condition substantially softens as the pulse grows and the amplification slows down. Therefore, even under conditions when the linear amplification stage is strongly affected by the pump fluctuations, the ultimate output pulse can be of high quality. This is illustrated by Fig. 4, which shows numerical results for initial and boundary conditions,

$$\varepsilon(y) = 0.1,$$

$$A(t,y) = 1 + \frac{0.5}{\sqrt{5}} \sum_{i=1,2,3,5,6} \cos\left(2\pi \left(\frac{y}{\Delta y} + \sqrt{i}\,\frac{2}{5} \right) - \sqrt{i}\,\frac{\omega t}{N} \right).$$

$$\Delta y = 5000\lambda, \quad N = 1200. \tag{22}$$

In this example, which models random pump fluctuations around the average amplitude a_0, the duration of fluctuations exceeds the linear BRA time $(a_0\sqrt{\omega\omega_p})^{-1}$, but is less than the total BRA time. Therefore, the pumped pulse acquires, during the linear BRA, a strong transverse intensity dependence corresponding to that of the not yet averaged pump. The transverse profile of the pumped pulse is smoothed then during nonlinear BRA due to the averaging of the pump fluctuations already met. Diffraction effects are negligible in this example because of a sufficiently large transverse fluctuation size Δy.

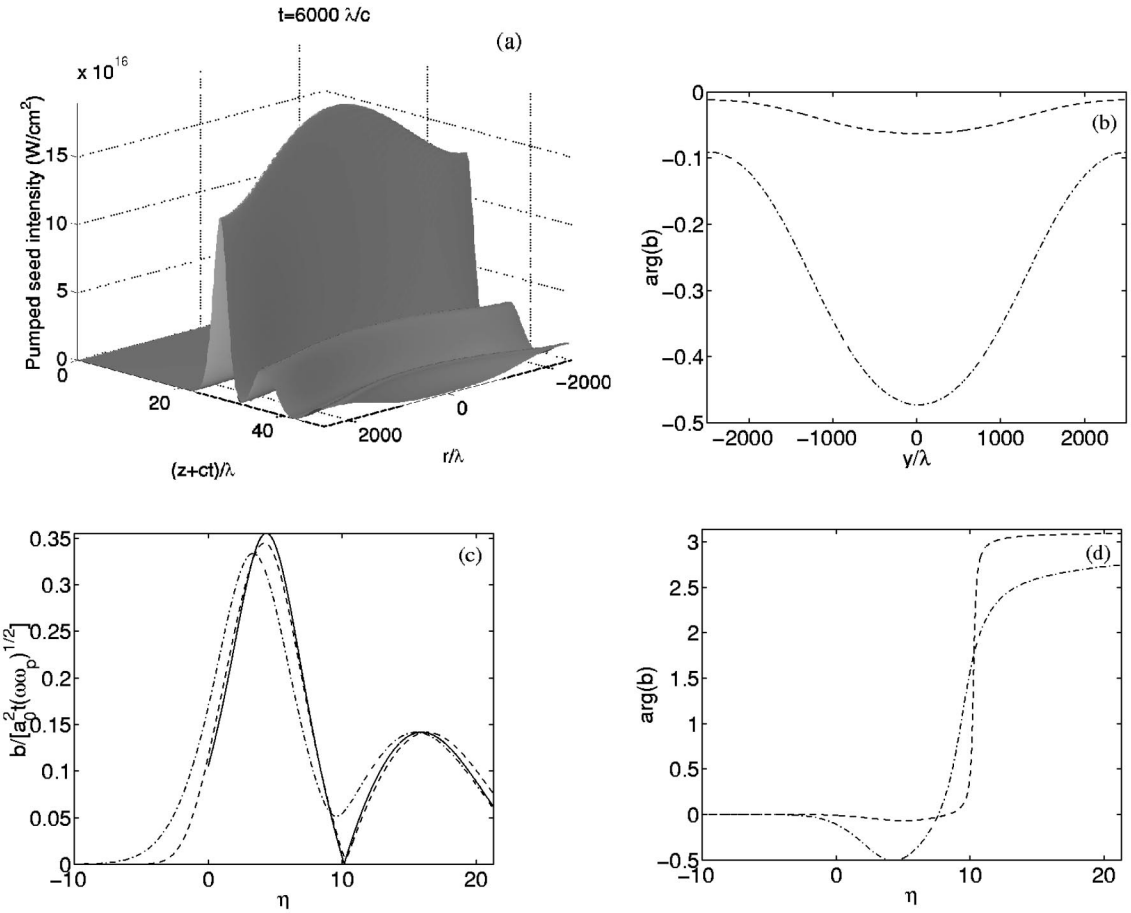

FIG. 6. The effects of the pumped pulse relativistic electron nonlinearity on BRA: (a) the distribution of pumped seed intensity; (b) the transverse dependence of the pumped pulse phase modulations for the z-location of the maximum pulse intensity at times $t=3000\lambda/c$ (dashed line) and $t=6000\lambda/c$ (dash–dotted line); (c), (d) the longitudinal dependences of the pumped pulse amplitude [(c) plot] and phase [(d) plot] for $y=0$. The dashed and dash–dotted lines correspond to the times $t=3000\lambda/c$ and $t=6000\lambda/c$, respectively. The solid line on the (c) plot shows the respective self-similar solution in the absence of the cubic nonlinearity.

For a much smaller transverse fluctuation size, $\Delta y=100\lambda$, the diffraction may somewhat transform the amplitude modulations of the pumped pulse into phase modulations. Such phase modulations may in turn produce the amplitude modulations that do not disappear even during the latest nonlinear stage of BRA. This is illustrated by Fig. 5. As discussed above, as long as the phase modulations are small, the output focusability is not spoiled.

VII. SELF-FOCUSING AND SELF-PHASE-MODULATION EFFECTS

In all of the earlier examples, we neglected self-focusing and self-phase-modulation effects. These effects limit, in fact, the allowed BRA duration. We consider now these limitations numerically by solving our basic equations for the actual nonzero value of δ. We take the same initial and boundary conditions as in the Sec. V treating the transverse modulations of the seed amplitude, namely,

$$\varepsilon(y)=0.1\left(1+0.5\cos\left(2\pi\frac{y}{\Delta y}\right)\right), \quad \Delta y=5000\lambda, \quad A(t,y)=1. \tag{23}$$

The results of the calculation, presented in Fig. 6, indicate that the relativistic electron nonlinearity does not significantly change the BRA dynamics up to the amplification time of about $6000\lambda/c$.

Note from Fig. 6(b) that the nonlinear focusing effects are clearly seen at $t=6000\lambda/c$, when the nonlinear phase shift becomes of order unity, which means that the local nonlinear focusing length becomes of the order of the pulse diffraction length. The output pulse can still be well focusable in vacuum with a focal length much smaller than this very large diffraction length. Since a noticeable portion of the pulse energy acquires transverse wave numbers $\sim 2\pi/\Delta y$, the focal spot radius becomes $\sim F\lambda/\Delta y$.

Figures 6(c) and 6(d) show the longitudinal dependence of the pumped pulse amplitude and phase.

The transverse self-focusing and longitudinal self-phase-modulation effects are caused by the nonlinear frequency shift, which is proportional to the local intensity of the seed pulse. This frequency shift increases $\propto t^2$ in the BRA process. The respective phase shift increases $\propto t^3$. If this extra phase shift between the pumped pulse front and maximum were to reach π, then the energy flow would be reversed back from the pulse to the pump and the leading spike could even split

in the longitudinal direction. The transverse dependence of the nonlinear phase shift deforms the phase fronts and could even cause the transverse filamentation of the pumped pulse. Both the longitudinal and the transverse filamentation effects are deleterious, so that the amplification should be accomplished before such effects develop.

VIII. CONCLUSION

We have shown that a prefocused pulse conserves its phase front if the diffraction length of the seed is much larger than the amplification length. This result might be used in practical applications to gain even higher laser intensities when the exiting pulse already has so large an intensity that it cannot be manipulated by ordinary means. What we show is that, by making a parabolic phase front with a weak seed, the phase front can be conserved under amplification, making possible the intense output focusing in vacuum.

We analyzed the stability of the backward Raman amplification to large scale perturbations of the seed and pump. Because of the weak dependence of the exiting pulse on the initial seed parameters, perturbations of the seed become smaller during the amplification process. Also, using an irregular pump gives results equivalent to an averaging of the random component. The exiting pulse retains its phase front.

We also determined numerically the amplification length for which self-focusing and self-phase-modulation effects do not spoil the output pulse quality.

We did not consider in this paper the important effects of plasma density fluctuations on BRA, since these effects require a very different treatment.

ACKNOWLEDGMENTS

Authors are thankful to A. A. Balakin and V. A. Mironov for help in numerical simulations and useful discussions.

The work is supported by the United States DARPA and the Russian Foundation for Basic Research (Grant No. 02-02-17275).

[1] V. M. Malkin, G. Shvets, and N. J. Fisch, Phys. Rev. Lett. **82**, 4448 (1999).
[2] G. A. Mourou, C. P. J. Barty, and M. D. Perry, Phys. Today **51** (1), 22 (1998); M. D. Perry, D. Pennington, B. C. Stuart *et al.*, Opt. Lett. **24**, 160 (1999).
[3] V. M. Malkin, G. Shvets, and N. J. Fisch, Phys. Plasmas **7**, 2232 (2000).
[4] A. G. Litvak, Zh. Eksp. Teor. Fiz. **57**, 629 (1969) [Sov. Phys. JETP **30**, 344 (1970)]; C. Max, J. Arons, and A. B. Langdon, Phys. Rev. Lett. **33**, 209 (1974); G.-Z. Sun and J. M. Finn, Phys. Fluids **30**, 526 (1987).
[5] W. L. Kruer, *The Physics of Laser Plasma Iteractions* (Addison-Wesley, Redwood City, CA, 1988), Chap. 7.
[6] Yu. A. Tsidulko, V. M. Malkin, and N. J. Fisch, Phys. Rev. Lett. **88**, 235004 (2002).
[7] V. M. Malkin, G. Shvets, and N. J. Fisch, Phys. Rev. Lett. **84**, 1208 (2000).
[8] J. R. Murray, J. Goldhar, D. Eimerl, and A. Szoke, IEEE J. Quantum Electron. **QE-15**, 342 (1979).